# MOLECULAR DYNAMICS SIMULATION OF NANO WETTING OF LENNARD-JONES DROPLET ON CURVED SURFACES

## SALEH IRSHEID SALEH ALHIASSAH

## UNIVERSITI SAINS MALAYSIA

2023

# MOLECULAR DYNAMICS SIMULATION OF NANO WETTING OF LENNARD-JONES DROPLET ON CURVED SURFACES

by

## SALEH IRSHEID SALEH ALHIASSAH

Thesis submitted in fulfilment of the requirements for the degree of Doctor of Philosophy

December 2023

#### **ACKNOWLEDGEMENT**

First of all, I would like to thank Almighty Allah for the many blessings He's bestowed upon me during my studies and in completing this thesis. May Allah's blessing goes to the final Prophets Muhammad peace be upon him, his family, and his companions. I would like to express my deep appreciation and gratitude to several individuals who have been instrumental in helping me complete this PhD thesis.

First and foremost, I would like to thank my supervisor, **PROFESOR MADYA DR. YOON TIEM LEONG**, for his unwavering support, guidance, and encouragement throughout my doctoral studies. His expertise, patience, and feedback have been invaluable to me and have helped me to grow both as a scholar and as a person. I am truly fortunate to have had him as my supervisor, and I am grateful for everything he has done for me.

I would also like to thank my family for their endless love, encouragement, and support. Their unwavering belief in me has kept me going through the many ups and downs of the PhD journey, and I am grateful for all the sacrifices they have made to help me pursue my dreams.

Finally, I would like to acknowledge the support of my friends and colleagues, whose camaraderie, encouragement, and advice have been invaluable to me over the years. I am grateful for the many stimulating conversations, collaborations, and shared experiences that have helped me to grow both personally and professionally.

Thank you all for your support, encouragement, and friendship. Your contributions have made this journey possible, and I could not have completed it without you.

## TABLE OF CONTENTS

ACK	KNOWLEDGEMENT	ii
TAB	LE OF CONTENTS	iii
LIST	Γ OF TABLES	vi
LIST	Γ OF FIGURES	vii
LIST	Γ OF SYMBOLS	xiii
LIST	Γ OF ABBREVIATIONS	xvi
LIST	Γ OF APPENDICES	xvii
ABS	TRAK	xviii
ABS	TRACT	xxi
СНА	APTER 1 INTRODUCTION	1
1.1	Introduction	1
1.2	Motivation	8
1.3	Problem statement	9
1.4	Objectives of study	10
1.5	Research gap and novelty	10
1.6	Scope of the study	11
1.7	Thesis outline	12
CHA	APTER 2 LITERATURE REVIEW	13
2.1	Introduction	13
2.2	Characterization of atomic behavior using MD simulation	13
2.3	Different computational approaches	20
2.4	Contact-angle and wetting characterization of triple surfaces	24
2.5	Surface characteristic energy	28
2.6	LJ potential of different surface geometries	30
2.7	Apparent line tension	38

2.8	Effect of	f the line curvature on surface	42
2.9	The inte	rfacial energy of droplets on various surfaces	47
2.10	Interfaci	al tension influenced by droplet size dependent contact angle	49
СНА	PTER 3	THEORETICAL BACKGROUND	55
3.1	A brief i	ntroduction to wetting phenomena	55
3.2	Classica	l theory of wetting	56
3.3	Theoreti	cal background of molecular dynamics	58
CHA	PTER 4	METHODOLOGY	63
4.1	Computa	ational method	63
	4.1.1	Stage 1: Configuration preparation	64
	4.1.2	Stage 2: Running MD simulations with the LAMMPS Package	70
		4.1.0( ) [7]	
		4.1.2(a) The input script	
		4.1.2(a)(i) Initialization	
		4.1.2(a)(ii) System definition	
		4.1.2(a)(iii) Simulation settings	
	4.1.3	Stage 3: Post-processing of simulation output	
СПУ	PTER 5	RESULTS AND DISCUSSION	
5.1	Thermal	equilibration	96
	5.1.1	Thermal equilibration of $\theta_w$ in configurations with a flat substrate	97
	5.1.2	Thermal equilibration of $\theta_w$ in configurations with a curved substrate	99
	5.1.3	Thermal equilibration of $R_c$	101
5.2		angle variation induced by geometry and the LJ characterizing end	
	5.2.1	Morphology and contact angle as a function of <b>K</b> at fixed LJ potential in the 2D configurations	.105
	5.2.2	Morphology and contact angle as a function of <b>K</b> at fixed LJ potential in the 3D configurations	.107

	5.2.3	Contact angle variation induced by LJ characterizing energy LJ at a fixed $R_{\rm sub}$	108
	5.2.4	Morphology and contact angle as a function of $\epsilon_{12}$ at fixed $R_{\mathrm{sub}}$ in the 2D configurations	109
	5.2.5	Morphology and contact angle as a function of $\epsilon_{12}$ at fixed $R_{\mathrm{sub}}$ in the 3D configurations	111
	5.2.6	Contact radius $R_c$ as a function of $K$ at fixed LJ potential	112
	5.2.7	Contact radius $R_c$ as a function of $\epsilon_{12}$ at fixed $R_{\mathrm{sub}}$	114
	5.2.8	Summary of numerical data for contact angle and radius obtained for all $\epsilon_{12}$ values	115
5.3	Line ten	sion	117
	5.3.1	Young's contact angle $\theta_Y$	117
	5.3.2	Evaluation of liquid-vapour surface tension $\sigma_{lv}$ of the LJ droplet	119
	5.3.3	Evaluation of line tension	121
CHA	PTER 6	CONCLUSION AND FUTURE WORK	125
6.1	Conclus	ion	125
6.2	Recomm	nendation for future work	128
REFI	ERENCES	S	130
APPF	ENDICES		

## LIST OF TABLES

	Page
Table 4.1	The initial parameters of the 3D configurations with curvature for the numerical experiments conducted in this thesis
Table 4.2	The initial parameters of the 2D configurations with curvature for the numerical experiments conducted in this thesis
Table 5.1	The parameters of the MD simulation display complete wetting (filled) scenario. Contact angle is not measured in these cases 105
Table 5.2	Summary of the parameters and numerical data obtained from all MD simulations with 2D configurations
Table 5.3	Summary of the parameters and numerical data obtained from all MD simulations with 3D configurations
Table 5.4	Young contact angle obtained via extrapolation as in Fig. (5.13) 119
Table 5.5	LJ droplet size-dependent values of line tension as calculated based on the data derived from the MD simulations performed in
	this thesis

## LIST OF FIGURES

	Page
Figure 1.1	Growing interest in using MD simulation to gain a better knowledge of the fundamentals of the coatings industry (Sethi, 2022)
Figure 1.2	A liquid adjacent to a solid surface has two equilibrium regimes: a partial wetting and a complete wetting. In the former case, three phases are in contact at the base line of the droplet (Krishnakumar, 2010)
Figure 1.3	Surface characterization using contact angle
Figure 2.1	Illustration of different simulation techniques conventionally employed for simulating polymeric materials and their behavior (Sethi, 2022)
Figure 2.2	Potential energy field perpendicular to the substrate surface under different conditions(non-wetting, partial wetting, and complete wetting) (Hubao <i>et al.</i> , 2020)
Figure 2.3	Hierarchy chart of computational approaches
Figure 2.4	The contact angles of droplets on the substrate
Figure 2.5	Wetting States of Water on Textured Surfaces: Cassie and Wenzel States. (a) The Cassie state where water droplets (red) sit on a cushion of air, only contacting the top of the surface texture (blue) without penetrating it. (b) The Wenzel state where water fully wets the surface texture, resulting in extensive contact between the water and the solid surface (Prakash <i>et al.</i> , 2016)
Figure 2.6	Lennard-Jones potential
Figure 2.7	Schematics of the curvature effect on the interactions between a single molecule and curved substrate

Figure 2.8	The wetting-drying boundary $\theta_{Yw}$ of detachable and wrapped spherical droplets (Iwamatsu, 2016b)
Figure 2.9	A cross-section of the droplet with a radius of curvature R and a base radius forming a contact angle $\theta$ with the surface (Kanduč <i>et al.</i> , 2018)
Figure 2.10	Snapshots of the simulation setups: (a) a spherical and (b) a cylindrical water droplet (simulation data from (Kanduč <i>et al.</i> , 2018)) on the surface
Figure 2.11	Typical conformations of dynamical equilibrium for Water Molecules on Pt-Surface (a) and C-Surface (b) (Zhu et al., 2018) 46
Figure 2.12	(a) Different contact angles of nanodroplets on concave walls with curvature. (b) Variation trend of line tension with curvature (Ma <i>et al.</i> , 2021b)
Figure 2.13	The existence of surface tension is due to intermolecular forces 48
Figure 2.14	Morphological evolution of a droplet placed on the bottom of a spherical cavity as the droplet volume is increased (Iwamatsu, 2016a)
Figure 2.15	Theoretical prediction and experimental measurement of apparent contact angle of liquid droplet on curved surfaces (Wu <i>et al.</i> , 2015)
Figure 4.1	The three distinct stages of numerical experiments
Figure 4.2	Labeled dimensions of the 3D flat, 2D flat, 3D (with curvature), and 2D (with curvature) configurations
Figure 4.3	Graph of temperature against time-steps of equilibration of Ar sphere
Figure 4.4	A sample output of the measurement of the diameter of an LJ spherical sphere at the end of equilibration
Figure 4.5	Graphical illustration of the preparation of (a), (b): The initial LJ spherical droplet and cylinder; (c), (d): The initial spherical shell

	and flat substrate; (e), (f): The initial cylindrical shell and flat strip substrate	73
Figure 4.6	The four different configuration types, namely, (a) 3D (b)3Df (c)2D and (d) 2Df	75
Figure 4.7	A flowchart of a typical MD algorithm	77
Figure 4.8	Graphical visualization of the spreading evolution of an LJ cylinder on the solid substrate at different stages in the 2D case with a non-zero curvature, $R_{\rm sub}$	82
Figure 4.9	Graphical visualization of the spreading evolution of an LJ column on the solid substrate at different stages in the 2Df case with a zero curvature, $R_{\rm sub}=0$	83
Figure 4.10	Graphical visualization of the spreading evolution of an LJ column on the solid substrate at different stages in the 3D case with a non-zero curvature, $R_{\rm sub}$	83
Figure 4.11	Graphical visualization of the spreading evolution of an LJ column on the solid substrate at different stages in the 3D case with a zero curvature, $R_{\text{sub}} = 0$	84
Figure 4.12	(a): Visualization of an LJ column on the inner curved surface of a cylindrical shell substrate. (b): Visualization of the same LJ droplet on the substrate with the substrate atoms hidden. Despite the absence of the substrate atoms, the boundary of the substrate on which the LJ column rests can be clearly inferred	
Figure 4.13	(a): A slice of thickness $\Delta t_{\rm slice}$ is cut out from an LJ droplet at an angle $\phi_j$ , where the x-axis penetrated the slice right through the middle of the thickness. (b): A slice of thickness $\Delta t_{\rm slice}$ is cut out from an LJ column along the y-axis at $y=y_j$ , where the y-axis penetrate the slices right through the middle	87
Figure 4.14	An example of an LJ slice with a thickness of $\Delta t_{\rm slice}$ cut out from an LJ droplet/column. The yellow dots represent the sparse atoms that are not attached to the bulk of the LJ droplet, while the black	

	removed	. 88
Figure 4.15	Schematic representation of the horizontal slicing method used to extract the atoms on the leftmost and rightmost surfaces of an LJ slice. The slice is first divided into $N_z$ equally thick horizontal slices, and the leftmost and rightmost atoms in each slice are identified based on their coordinates in the $x-y$ plane. The collection of all leftmost atoms forms the data points for the liquid-solid interface, while those of the rightmost atoms form the data points for the liquid-gas interface	. 90
Figure 4.16	AN LJ slice with sparse atoms removed. The dots on the left curve represent the liquid-solid interface, while those on the right represent the liquid-gas interface. The atoms on the liquid-solid interface are fitted using a spline, which is displayed in the form of a continuous curve. The spline interpolated through the atoms on the liquid-gas interface is not displayed.	. 90
Figure 4.17	The slopes and angles at the upper intersection point $(x_{peg}, y_{peg})_u$ . $R_c$ marks the contact radius, while $R_{sub}$ marks the best-fit value obtained by fitting the LJ atoms on the lm surface on the circle	
Figure 4.18	$(x_i - h_{\rm sub})^2 + (y_i - k_{\rm sub})^2 = R_{\rm sub}^2$ .  Typical graphical output produced by measure_angle.py.  Left: Configuration with a curve substrate. Right: Configuration with a flat substrate.	
Figure 5.1	(a) The contact angle vs. time of a two-dimensional droplet ( $r_d = 10 \text{ nm}$ ) spreading on a flat surface for three LJ characteristic energy, $\epsilon_{12}$ ; (b) Contact angle vs. time for the 3Df configuration	. 98
Figure 5.2	(a) The contact angle vs. time of a two-dimensional droplet ( $r_d$ = 10 nm) spreading on a curved surface for three LJ characteristic energy, $\epsilon_{12}$ ; (b) Contact angle vs. time for the 3D configuration with a curve substrate	100

Figure 5.3	(a) The contact radius $R_c$ vs. time of a two-dimensional droplet $(r_d = 10 \text{ nm})$ spreading on a flat surface for three LJ characteristic	
	energy, $\epsilon_{12}$ ; (b) Contact radius vs. time for the 3D configuration with a flat substrate	103
Figure 5.4	(a) The contact radius $R_c$ vs. time of a two-dimensional droplet $(r_d=10 \text{ nm})$ spreading on a curved surface for three LJ characteristic energy, $\epsilon_{12}$ ; (b) Contact radius vs. time for the 3D configuration with a curved substrate	103
Figure 5.5	Evolution of a typical LJ droplet's morphology during the MD simulation in a curved shell. The time sequence progresses from left to right	104
Figure 5.6	The contact angle $\theta_w$ versus $K$ for different sizes of droplets in a 2D. All the data points shown in the figure were obtained with the LJ characteristic energy $\epsilon_{12}$ set at the value of $1.0\epsilon_{12,\mathrm{std}}$	106
Figure 5.7	Illustration of an LJ droplet filling up the entire cavity wall when <i>K</i> is large in (a) 2D and (b) 3D	107
Figure 5.8	The contact angle $\theta_w$ versus $K$ for different sizes of droplets in a 3D. All the data points shown in the figure were obtained with the LJ characteristic energy $\epsilon_{12}$ set at the value of $1.0\epsilon_{12,\mathrm{std}}$	108
Figure 5.9	(a) Contact angle of 2D droplets (column of LJ droplets) at three characteristic energies on a solid cylindrical shell. The substrate radius is $R_{\rm sub}=9$ nm, 10.3 nm, 11 nm, and 11.7 nm. (b) a flat substrate	110
Figure 5.10	(a) Contact angle of 3D (spherical) droplets at three characteristic energies in a solid spherical shell. The substrate radius is $R_{\rm sub} = 7.2$ nm, 8 nm, 9.2 nm, and 10.2 nm. (b) A flat substrate	111
Figure 5.11	(a) The contact radius $R_c$ versus $K$ for different sizes of droplets in a 2D and (b) 3D shell. The LJ characteristic energy $\epsilon_{12}$ was set at the same value as that in Fig. (5.6) and Fig. (5.8), i.e., $1.0\epsilon_{12,\mathrm{std}}$	113
Figure 5.12	The contact radius $R_c$ at three characteristic energies for different sizes of droplets in (a) a cylindrical (2D) and (b) spherical (3D)	

	shell. The values of $R_{\text{sub}}$ are the same as that in Fig. 5.9 and Fig. 5.10
Figure 5.13	The variation of the cosine of the droplet contact angle with the
	droplet curvature $1/r_d$ at two characteristic energies, for both 2D
	and 3D droplets. The figures also include the extrapolated values
	for the Young contact angle
Figure 5.14	Simulation box for measuring LJ droplet liquid-vapour surface
	tension
Figure 5.15	The plot of $\cos \theta_w$ vs. $\frac{1}{R_c}$ using the data points for the 3D
	configuration, measured at a common value of $\epsilon_{12} = 1.0\epsilon_{12, \text{std}} \dots 121$
Figure 5.16	The plot of $\cos \theta_w$ vs. $\frac{1}{R_c}$ using the data points for the 2D
	configuration, measured at a common value of $\epsilon_{12} = 1.0\epsilon_{12, \text{std}} \dots 122$
Figure 5.17	$\tau$ vs. $r_d$ for 2D and 3D configuration at $\epsilon_{12} = 1.0 \epsilon_{12, \text{std}}$

#### LIST OF SYMBOLS

 $\theta_w$  Contact angle

 $\varepsilon_{O-S}$  Potential energy between oxygen atom and solid atoms

 $\varepsilon_{sf}$  Energy parameter of solid-fluid interaction potential

 $\varepsilon$  Energy parameter

 $\sigma_{sf}$  length parameter of solid- fluid

 $\sigma$  length parameter

K Kelvin

Degree

γ Interfacial tension

au Line tension

 $V_{ij}$  Interactions between atoms i and j

 $r_{ij}$  Interatomic spacing between atoms i and j

F Force

∇ Gradient

*H* Mean curvature of the substrate

*h* Distance

 $\delta_T$  Tolman length

 $\theta_{YW}$  Wetting-drying boundary

 $\rho_{180}$  Radius (volume)

 $\theta_Y$  Young's contact angle

 $au_{app}$  Apparent line tension

N Newton's force

R Curvature radii

*k* Curvature ratio

 $v_{dry}$  Droplet volume ratio at drying transition

 $v_{wet}$  Droplet volume ratio at wetting transition

U Total potential

 $\ddot{r}_{i}$  Particle's acceleration

m Mass

 $f_{ij}$  Force exerted on particle i by it interacts with particle j.

t Time

v(t) Velocity

 $\ddot{r}$  The rate of change of acceleration (Jerk)

 $\Omega$  Sub volume

*T* Temperature

 $k_B$  Boltzmann constant

P Pressure

 $\rho$  Density

Å Angstrom

ps Picosecond

Ar Argon

Cu Cuprum

eV Electron Volte

ns Nanosecond  $(10^{-9}s)$ 

 $M \hspace{1cm} 10^6$ 

 $n_b$  Timestep

s.d. Standard deviation

 $m_{\rm lm}$  Slope at leftmost

 $m_{\rm rm}$  Slope at rightmost

 $N_{2D}(\rho)$  Number density of atoms in the 2D plane

 $\epsilon_{
m 12,std}$  The reference well depth of the LJ potential

 $R_{\rm sub}$  Substrate curvature

 $R_c$  Contact radius

 $r_d$  Initial radius of droplet

 $r_{tmp}$  Droplet radius at the end stage of the equilibration

 $t_{ck}$  Thickness

#### LIST OF ABBREVIATIONS

LAMMPS Large-scale Atomic/Molecular Massively Parallel Simulator

MD Molecular Dynamic

MC Monte Carlo

LJ Lennard-Jones

MM Molecular mechanics
QM Quantum mechanical

DFT Density functional theory

QMD Quantum molecular dynamics

SNFND Sessile nanofluid nanodroplet

 $Cyl_{app}$  Cylindrical apparent line tension

Sphane Spherical apparent line tension

NVE Constant number (N), volume (V), and energy (E)

NVT Constant number (N), volume (V), and temperature (T)

Rm Rightmost
Lm Leftmost

VMD Visual Molecular Dynamics

FFs Fixed-charge force fields

Fcc Face centered cubic

MPI Message Passing Interface

HPC High-performance computing

GPU Graphical processing units

### LIST OF APPENDICES

Appendix A trim\_measure\_ball\_column\_eq\_v2.wl

Appendix B in.Ar.metal.fpf.2D

Appendix C in.Cu.metal.cuboid\_v8

Appendix D gen\_geometries\_Cu\_v17.sh

Appendix E merge\_v18.sh

Appendix F in.ppp\_v14\_11

Appendix G measure\_angle.py

Appendix H functions.py

Appendix I appendrecord.cvs

Appendix J abstract\_csv.py

Appendix K appendrecord\_processed.csv

Appendix L wa\_dist\_1.png

Appendix M wa\_dist\_2.png

# SIMULASI DINAMIK MOLEKUL PEMBASAHAN NANO BAGI TITISAN LENNARD-JONES PADA PERMUKAAN MELENGKUNG

#### **ABSTRAK**

Pada skala nano, tingkah laku membasahkan titisan cecair pada permukaan pepejal berbeza disebabkan oleh ketegangan garisan  $(\tau)$  dan kesan nano lain, boleh diabaikan pada skala makroskopik. Ketegangan talian terhasil daripada variasi dalam ketumpatan tenaga antara muka antara talian sentuhan tiga fasa dan antara muka cecair-wap. Ia lebih ketara dalam konfigurasi 3D dengan kelengkungan bukan sifar, seperti titisan Lennard-Jones (LJ) pada permukaan sfera, berbanding dalam tetapan 2D seperti titisan lajur silinder tak terhingga pada permukaan silinder dengan talian sentuhan kelengkungan sifar. Selain itu, pada skala nano, morfologi titisan dan pembasahan pada substrat melengkung berbeza dengan ketara apabila kelengkungan berbeza menyumbang dengan ketara, berbeza dengan substrat rata. Sukar untuk mendapatkan gambaran lengkap tentang tingkah laku umum nanodroplet pada permukaan berstruktur menggunakan pendekatan eksperimen atau teori semasa. Salah satu sebab utama kesukaran ini adalah disebabkan saiz fenomena pembasahan nano yang sangat kecil yang secara teknikalnya dicabar untuk diukur. Khususnya, pengukuran kesan tegangan garisan dalam fenomena pembasahan titisan nano telah diketahui membawa kepada keputusan yang tidak konsisten disebabkan oleh pelbagai kesukaran teknikal, seperti ketidakteraturan pada permukaan substrat, pencemaran, kesan graviti dan lain-lain. Tesis ini bertujuan untuk menyiasat tingkah laku pembasahan Titisan nano LJ pada permukaan melengkung menggunakan simulasi dinamik molekul (MD) yang dilaksanakan dalam pakej Simulator Selari Atom/Molekul Berskala Besar (LAMMPS). Metodologi yang dicadangkan tidak

mengalami masalah teknikal yang melanda pendekatan eksperimen. Tesis ini memberi tumpuan kepada pengaruh geometri permukaan melengkung dan potensi interaksi LJ yang berbeza-beza terhadap peralihan pembasahan. Konfigurasi terdiri daripada titisan sfera LJ dalam interaksi dengan permukaan melengkung dalam bagi cangkerang sfera pepejal (konfigurasi 3D) dan titisan silinder LJ dalam interaksi dengan permukaan melengkung dalam bagi cangkerang silinder pepejal (konfigurasi 2D). Medan daya yang digunakan dalam simulasi MD hanya mengambil bentuk LJ prototaip, iaitu V = $4\epsilon \left[\left(\frac{\sigma}{r}\right)^{12} - \left(\frac{\sigma}{r}\right)^{6}\right]$ . Sistem yang dimodelkan dalam tesis ini adalah susunan magnitud yang lebih besar daripada yang terdapat dalam banyak simulasi MD sebelumnya. Secara khusus, bilangan atom yang terlibat dalam beberapa konfigurasi, terutamanya dalam 3D, adalah lebih kurang ~106. Di samping itu, pemprosesan pasca data daripada simulasi untuk mendapatkan kuantiti fizik yang berkaitan adalah teliti dan direka bentuk secara sengaja untuk meningkatkan kebolehpercayaan statistik bagi nilai akhir yang dilaporkan. Kesan pekali  $K=r_d/R_{\mathrm{sub}}$ \_sub pada morfologi titisan dan tegangan garisan dalam titisan nano yang berinteraksi dengan dinding pepejal cekung diperiksa menggunakan potensi LJ dengan kedalaman telaga  $\epsilon_{12, \mathrm{std}} = 0.003$  eV. Berdasarkan keputusan eksperimen berangka yang dijalankan dalam tesis ini, didapati fenomena pembasahan titisan LJ dalam konfigurasi 3D adalah serupa dengan rakan 2D yang sepadan. Walau bagaimanapun, arah aliran sudut sentuhan  $(\theta_w)$  hanya menunjukkan sedikit perbezaan apabila K berubah daripada  $K_1$  kepada  $K_2$ . Dalam kes 2D,  $\theta_w$  meningkat sedikit, manakala dalam kes 3D,  $\theta_w$  menurun sedikit apabila Kberubah daripada  $K_1$  kepada  $K_2$ . Peralihan morfologi cembung-rata-cekung permukaan titisan yang disebabkan oleh variasi dalam tenaga ciri LJ berjaya disimulasikan.  $\tau$  bagi konfigurasi 3D dan rakan 2D yang sepadan telah diukur dan dibandingkan menggunakan data daripada simulasi MD. Keputusan pengukuran, di mana au adalah dalam susunan magnitud  $\sim 10^{-10}$  N, adalah konsisten dengan penemuan yang dilaporkan dalam literatur.

# MOLECULAR DYNAMICS SIMULATION OF NANO WETTING OF LENNARD-JONES DROPLET ON CURVED SURFACES

#### **ABSTRACT**

At the nanoscale, wetting behavior of a liquid droplet on a solid surface differs due to line tension  $(\tau)$  and other nano effects, negligible on macroscopic scales. Line tension results from variations in interfacial energy density between the three-phase contact line and the liquid-vapor interface. It is more pronounced in 3D configurations with non-zero curvature, like a Lennard-Jones (LJ) droplet on a spherical surface, than in 2D setups like an infinite cylindrical column droplet on a cylindrical surface with a zero-curvature contact line. Additionally, at the nano scale, droplet morphology and wetting on a curved substrate vary significantly when different curvatures contribute substantially, contrasting with flat substrates. It is difficult to gain complete insight into the general behavior of nanodroplets on structured surfaces using current experimental or theoretical approaches. One of the major reasons for this difficulty is due to the extremely tiny size of nano wetting phenomena that are technically challenged to measure. In particular, measurement of line tension effect in nano droplet wetting phenomena has been known to lead to inconsistent results due to various technical difficulties, such as irregularity on the substrate surface, contamination, gravitational effects etc. This thesis aims to investigate the wetting behavior of LJ nanodroplets on curved surfaces using molecular dynamics (MD) simulations implemented in the Large-scale Atomic/Molecular Massively Parallel Simulator (LAMMPS) package. The proposed methodology does not suffer the technical issues that plague experimental approaches. The thesis focuses on the influence of curved surface geometry and varying LJ interaction potentials on wetting transitions. The

configurations consist of an LJ spherical droplet in interaction with the inner curved surface of a solid spherical shell (3D configuration) and an LJ cylindrical droplet in interaction with the inner curved surface of a solid cylindrical shell (2D configuration). The force field used in the MD simulation takes only a prototypical LJ form, namely  $V = 4\epsilon \left[ \left( \frac{\sigma}{r} \right)^{12} - \left( \frac{\sigma}{r} \right)^{6} \right]$ . The system modeled in this thesis is orders of magnitude larger than those in many previous MD simulations. Specifically, the number of atoms involved in some configurations, especially those in 3D, is approximately  $\sim 10^6$ . In addition, the post-processing of the data from the simulation to obtain the relevant physical quantities is rigorous and purposely designed to enhance the statistical reliability of the final reported values. The impact of the  $K=r_d/R_{\rm sub}$  coefficient on droplet morphology and line tension in nanodroplets interacting with concave solid walls are examined using the LJ potential with a well depth of  $\epsilon_{\rm 12,std} = 0.003$  eV. Based on the results of the numerical experiments conducted in this thesis, it is found that the wetting phenomena of an LJ droplet in 3D configurations are similar to those of its corresponding 2D counterparts. However, the trend of contact angle  $(\theta_w)$  showed only a slight difference when K changed from  $K_1$  to  $K_2$ . In the 2D case,  $\theta_w$  increased slightly, whereas in the 3D case,  $\theta_w$  decreased slightly when K changed from  $K_1$  to  $K_2$ . A convex-flat-concave morphology transition of a droplet surface induced by the variation in the LJ characteristic energy was successfully simulated. The  $\tau$  of 3D configurations and their corresponding 2D counterparts was measured and compared using data from the MD simulations. The measurement results, where the  $\tau$  is in the order of magnitude of  $\sim 10^{-10}$  N, are consistent with the findings reported in the literature.

#### **CHAPTER 1**

#### INTRODUCTION

#### 1.1 Introduction

Droplet wetting on a solid substrate surface is a fundamental and important phenomenon that has gained increasing attention in the scientific community. The behavior of droplets on a surface is influenced by the interaction between the droplet, the substrate, and the surrounding environment. Understanding this phenomenon is critical in various fields such as materials science, physics, chemistry, engineering, and biology (Kim *et al.*, 2016, Wang *et al.*, 2022b, Mohammad Karim, 2022).

In this study, we will discuss the importance of droplet wetting phenomena on a solid substrate surface and its applications in various fields. Wetting is defined as the ability of a liquid to spread or adhere to a solid surface (LaPorte, 1997). This phenomenon is governed by the balance between the adhesive and cohesive forces of the liquid and the solid surface, respectively. When the adhesive forces are greater than the cohesive forces, the liquid will spread over the surface, resulting in a wetting phenomenon.

On the other hand, when the cohesive forces are greater, the liquid will form droplets, resulting in a non-wetting phenomenon. Droplet wetting behavior is influenced by several factors such as the surface roughness, chemical composition, and surface energy of the substrate, as well as the surface tension, viscosity, and contact angle of the droplet. These factors can be manipulated to control the wetting behavior and achieve specific functionalities. Wetting of liquid droplets is a fundamental physical process in many scientific and technical domains, including microfluidic,

nanofluidic, and nano printing. In fact, Galileo's report from 1612 contains his findings from the first study of wetting phenomena (Drake and Galilei, 1981).

Utilizing wetting and drying procedures inspired by biological structures, such as detergents, emulsions, textile dye processing, and chemical processing, has the potential to create novel materials using the biomimetics design concept (Drake and Galilei, 1981, Gennes *et al.*, 2004). Additionally, a greater understanding of wetting is crucial for fluids contained in nanoscale structures (Gennes *et al.*, 2004), as it can enable the development of smart surfaces and nano-based devices by manipulating wettability at the nanoscale.

The understanding and control of droplet wetting behavior has numerous applications in various fields. In materials science, it is used in the fabrication of self-cleaning surfaces, anti-fogging coatings, and superhydrophobic surfaces (Konar *et al.*, 2020, Nyankson *et al.*, 2022, Khan *et al.*, 2022), as shown in Fig. (1.1).

These surfaces can find applications in the automotive, aerospace, and marine industries, as well as in medical devices, where the prevention of bacterial adhesion is critical (Achinas *et al.*, 2019, Villegas *et al.*, 2019, Das and Mahanwar, 2020).

In the field of microfluidics, droplet wetting behavior is used to control the flow of fluids in microchannels. This technology has applications in lab-on-a-chip devices, where small volumes of fluids are manipulated for various analytical and diagnostic purposes.

In addition, droplet wetting behavior is crucial in the production of inkjet and 3D printing technologies. The precise control of droplet deposition on a surface is critical for achieving high-resolution prints and accurate 3D structures (Jafari *et al.*, 2019, Li, 2020, Arzt *et al.*, 2021, Zhou *et al.*, 2022).

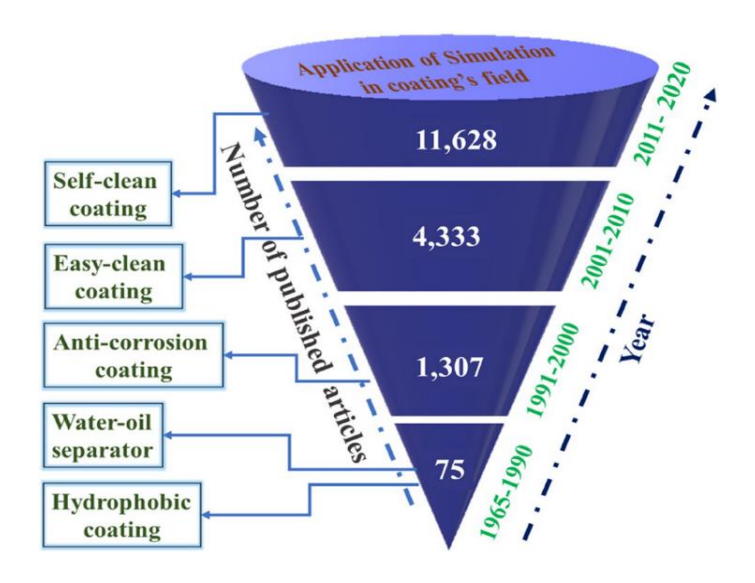


Figure 1.1. Growing interest in using MD simulation to gain a better knowledge of the fundamentals of the coatings industry (Sethi, 2022).

Typically, wetting deals with the three states of materials: solid, liquid, and gas. When the intermolecular interactions between solid and liquid are balanced, a liquid drop occurs at the solid/liquid/gas inter line with a contact angle of  $(\theta)$  (Gennes et al., 2004, Erbil, 2006, Butt et al., 2013, Bormashenko, 2018).

Generally, the creation of contact angles is determined by various factors, including the thermodynamic parameters of the liquid droplets and the substrate. Moreover, when a drop is beginning to wet a substrate, the contact angle will reach its maximum value (Krainer and Hirn, 2021).

When a liquid drop is placed on a solid surface, it can exhibit one of two unique behaviors: partial wetting, in which the drop creates a finite contact angle with the surface, or complete wetting, in which the contact angle is vanishing ( $\theta = 0$ ) (Leger and Joanny, 1992), as shown in Fig. (1.2).

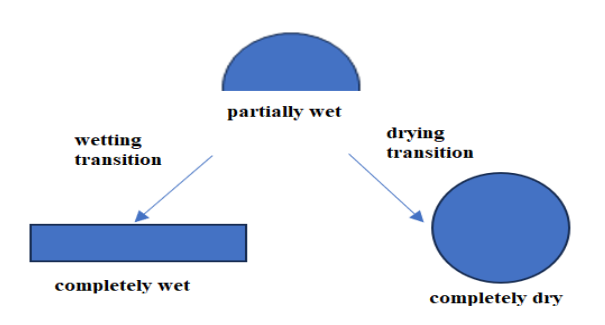


Figure 1.2. A liquid adjacent to a solid surface has two equilibrium regimes: a partial wetting and a complete wetting. In the former case, three phases are in contact at the base line of the droplet (Krishnakumar, 2010).

Therefore, the ultimate form of the drop is determined by the liquid's attraction to both it and a solid surface. If the liquid is significantly more attracted to itself than it is to the surface, which is hydrophobic in nature, the drop will "bead up" and create a large contact angle. While it will "spread out" and provide a low contact angle when the attraction to the surface is greater than the attraction to itself (Shen *et al.*, 2005), as shown in Fig. (1.3).

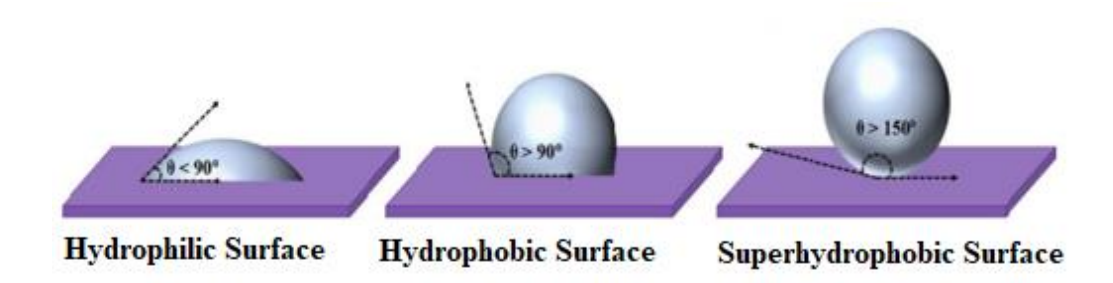


Figure 1.3. Surface characterization using contact angle.

The wettability of a solid surface is an essential property that affects a solid surface's ability to absorb droplets (Krainer and Hirn, 2021). Superhydrophobic surfaces are also utilized in a range of applications such as lotus leaf self-cleaning, strider leg hair, anti-icing surfaces, and improved phase change heat transfer surfaces (Shahraz *et al.*, 2012). The most essential way to change the wetting behavior is to alter the surface geometries rather than just using two different fluids. This ultimately

results in various wetting behaviors for each surface. Although, a droplet with a cylindrical morphology is a two-dimensional equivalent of a spherical (cap-shaped) droplet; it is also characterized as a liquid channel, filament, ridge, or bridge. In microfluidic devices, one of the most essential wetting morphologies is represented by the cylindrical droplet shape, which has important implications (Gau *et al.*, 1999, Brinkmann and Lipowsky, 2002, Brinkmann *et al.*, 2005, Mechkov *et al.*, 2007).

The cylindrical droplet shape is occasionally used in theoretical investigations for at least two additional reasons, including due to the removal of one spatial dimension, and the theoretical treatment is made simpler. It is possible to minimize the droplet's axial box size in computer simulations, which lowers the cost of calculations (Scocchi *et al.*, 2011, Vanzo *et al.*, 2012, Kanduč, 2017).

Generally, line tension must be dependent on the contact angle as well as the geometry of the solid-liquid, liquid-fluid, and solid-fluid interfaces (Marmur, 2006). In addition to being affected by line tension at the sessile droplet, contact angles also play a critical role in the stability of droplets and liquid deposits with diverse morphologies.

As a result, understanding line tension is essential for a variety of situations in many scientific and technological domains, with several applications including lubrication, painting, surface coating, oil recovery, and so on (Shen *et al.*, 2005).

To be more specific it is important to first define the two- and three-dimensional systems as well as the corresponding line tensions. This is due to the utilization of the line tension in both systems. A two-dimensional system contains at least two primary phases that aren't divided by surfaces but rather by lines. When all major phases are distinguished by interfaces, a system is said to be three-dimensional.

In two-dimensional systems, short-range forces are the most crucial, while in three-dimensional systems, long-range forces may be the more crucial or equally critical. Due to the role performed by the system's free energy influences on the heterogeneous nucleation (Joanny and De Gennes, 1986, Law, 1994, Retter *et al.*, 1996, Lefevre *et al.*, 2004), vaporization (Fan, 2006, Zhang *et al.*, 2014, Paneru *et al.*, 2015), spreading, and fragmentation of droplets (Aronson *et al.*, 1994, Brinkmann *et al.*, 2005, Guzzardi *et al.*, 2006, Mechkov *et al.*, 2007, Guillemot *et al.*, 2012).

As well as, stability of foams, films, filaments, droplets, nanobubbles, and even hydrophobic contacts are all affected (Wang et al., 2020b, Li et al., 2020a). The primary indicator for assessing a solid surface's wettability is the contact angle which is typically defined to describe the behavior of a liquid droplet on a solid surface and introduced as an angle between the tangent at the three-phase point and the solid surface (Brinkmann and Lipowsky, 2002, Mechkov *et al.*, 2007, Scocchi *et al.*, 2011). Generally, the contact angle, contact line radius, and line tension are the three most crucial variables that are utilized to characterize wetting behavior in addition to surface tension (Vanzo *et al.*, 2012).

Insufficient experimental and theoretical approaches persistently hinder the measurement and interpretation of contact angles, despite the apparent conceptual simplicity and extensive history of studies in this field (Bormashenko, 2018, Kanduč, 2017). Young's equation is known as the first attempt to quantify the contact angle. It provides an excellent macro-scale approximation of the contact angle but performs poorly when used to predict the micro- and nano-scale regimes (Marmur, 2006, Zhang et al., 2018). Recently, MD model have been proven as a useful technique for analyzing the wetting properties of nanodroplets on surfaces, spreading behaviors, and interfacial properties (Barisik and Beskok, 2014). Furthermore, this simulation

technique can be employed to explore the influence of various factors, including temperature, chemical composition, and surface roughness, on the wetting behavior of the droplet.

The use of simulations can offer valuable insights into the molecular-level behavior of fluids, aiding in the development of channels with specific properties that allow for the control of fluid flow and mixing. Additionally, simulations can be utilized in the design of surfaces that possess superhydrophobic or superhydrophilic properties, which are effective in producing self-cleaning surfaces and anti-fouling coatings (Drelich and Marmur, 2014). Another application of simulations is the investigation of surface wetting behaviors in extreme environments, such as high-pressure and high-temperature settings (Wang *et al.*, 2022a).

In recent years, the scientific world has given this topic increasingly more attention and many studies have been carried out. However, a fundamental comprehension of how substrate hydrophilicity and spreading are impacted by solid-liquid interactions is currently lacking (Aronson *et al.*, 1994, Fan, 2006, Paneru *et al.*, 2015). Researchers primarily concentrated on the wettability of specific materials under specific conditions, and the research objects were virtually flat surfaces, while the surface structure affects wettability. Therefore, it is crucial to research how solid-liquid interactions affect the liquid spreads on varies solid surfaces (Drake and Galilei, 1981, Guzzardi et al., 2006, Weijs et al., 2011, Guillemot et al., 2012, Wang et al., 2020b, Li et al., 2020a).

In this thesis, we focus on molecular simulations of wetting properties to investigate the spreading of droplets with the size-dependent contact angle and different LJ interaction potential with different geometries. Computational methods,

such as molecular dynamics (MD), can accurately quantify droplet morphology and systematically model nano-wetting to show how the geometry of a surface affects the spreading of a nano droplet on a substrate. Therefore, more research efforts have been focused on wetting transitions in 3D surfaces (Kanduč *et al.*, 2018, Ma *et al.*, 2021b). This study aims to investigate wetting transitions with different geometries by changing curvature ratios with constant Lennard-Jones (LJ) for different nanodroplet sizes. Furthermore, to examine the effect of interaction potential on nanodroplet morphologies, varying LJ values were manipulated with fixed curvature ratios in both 2D and 3D.

#### 1.2 Motivation

The motivation for performing MD simulations on nano wetting phenomena on a curved solid substrate surface is to understand the complex behavior of droplets on surfaces with different geometries. Curved surfaces, such as nanowires, nanopillars, and nanoparticles, have unique wetting properties compared to planar surfaces, which can affect their behavior in various applications, such as in microfluidics, nanosensors and surface coatings. MD simulation can provide detailed information on the wetting behavior of droplets on curved surfaces, such as the contact angle, line tension, spreading coefficient, surface energies, which can be difficult to measure experimentally. The simulation can also be used to investigate the effect of various factors, such as the radius of curvature, surface roughness, and chemical composition, on the wetting behavior of droplets on curved surfaces. Understanding the wetting behavior of droplets on curved surfaces is important for designing and optimizing the performance of various devices and materials at the nanoscale. For example, in microfluidics, the behavior of droplets on curved surfaces can affect the flow of fluids and the mixing of fluids, which is important for designing high-performance

microfluidic devices. In nanosensors, the wetting behavior of droplets on curved surfaces can affect the sensitivity and selectivity of the sensor, which is important for detecting specific molecules and analytes. In short, performing MD simulations on nano wetting phenomena on a curved solid substrate surface can provide valuable insights into the behavior of droplets on surfaces with different geometries, which is important for designing and optimizing various devices and materials (Ma *et al.*, 2021a, Macko *et al.*, 2022).

#### 1.3 Problem statement

The current literature lacks a comprehensive understanding of the curvaturedependence of wetting transitions in molecular dynamics simulations (Marmur, 2006, Zhang et al., 2018). It has been shown that droplet morphology on spherical surfaces can differ significantly from that on flat substrates when the contribution of different curvatures is non-negligible. In contrast to the size-independent contact angle defined by the modified classical Young's equation in macroscopic behavior (Krainer and Hirn, 2021), the wetting behavior of a liquid droplet on a solid surface significantly diverges at the nanoscale. Despite the importance of droplet size and wetting phenomena on structured surfaces, such as solid curved surfaces, experimental and theoretical studies are limited due to the apparent obstacles of conducting measurements at this scale. Moreover, while the well-known issue of surface tension's dependency on curvature continues to pique people's curiosity (Fan, 2006, Zhang et al., 2014, Paneru et al., 2015), it is difficult to gain complete insight into the general behavior of nanodroplets on structured surfaces using current experimental or theoretical approaches. One of the major reasons for the difficulty is due to the extremely tiny size of the nano wetting phenomena that are technically challenged to measure. In particular, measurement of line tension effect (Amirfazli et al., 2004) in nano droplet wetting phenomena has been known to lead to inconsistent results due to various technical difficulties, such as irregularity on the substrate surface, contamination, gravitational effects etc. Such practical problems can be best answered by using complementary computational approaches such as MD.

#### 1.4 Objectives of study

- To develop an original package of computational code to statistically measure
  the contact angle of the LJ droplets on the substrate as a function of different
  LJ interaction strength for the MD data obtained.
- 2. To examine quantitatively how the transition of wetting angle can be induced by manipulating the LJ interaction strength, droplet size, and substrate curvature at the nanoscale.
- 3. To gain a molecular-level understanding of the factors that govern the wetting behavior of LJ droplets on curved substrate surfaces at the nanoscale.

#### 1.5 Research gap and novelty

This thesis focuses on the wetting transition of LJ nanodroplets and the influence of curved surface geometry, using molecular dynamics simulations. It aims to address the gap in literature by contributing new numerical measurements for understanding the complex behavior of wetting phenomena at the nanoscale. To this end, both the design of surface and droplet are important. While some previous studies have investigated wetting transitions of LJ nanodroplets in 3D, there is currently not much research that explores the effects of varying LJ interaction potentials, curvature ratios, and droplet sizes on wetting transitions in both 2D and 3D and compares them. This thesis aims to fill this gap by measuring the contact angles, contact radius and line tension of a 2D and 3D LJ droplet on curved surfaces at different LJ characteristic

energy and comparing them. The results of this study will provide insights into the effects of varying LJ interaction potentials, curvature ratios, and droplet sizes on nano wetting transitions in both 2D and 3D.

This thesis introduces two novelties in the field of molecular dynamics simulations of LJ droplets. Firstly, the size of the systems modelled with LAMMPS is orders of magnitude larger than those in many previous MD simulations of LJ droplets. Specifically, the number of atoms involved in some configurations, especially those in 3D, is approximately  $\sim 10^6$ , which is considered very large from the viewpoint of previous MD simulations of similar nature such as (Hong et al., 2009) where the number of atoms is around  $\sim 10^4$ . Secondly, this thesis uses home-grown numerical codes mostly written in Python and Shell scripts for post-processing the MD data to extract contact angles, contact radius and other relevant quantities. The method of measuring these physical quantities from the MD data is unique and rigorous. The thesis does not make use of any pre-made packages developed or provided by any third party. In particular, a single contact angle value reported for an MD simulation of a configuration equilibrated for 2M steps is obtained by averaging approximately  $\sim 10^2$ measurements that are statistically sampled from a series of different time frames. The samples were filtered to omit possible outliers to enhance the reliability of the contact angle that is reported as the final figure.

#### 1.6 Scope of the study

The methodology deployed in this thesis involves only theoretical study and application of computational approaches, including application of computer software and programming techniques, while no experimental works will be performed. MD will be used as the computational tool for performing numerical experiments of nano

wetting phenomena in place of real-life experiments that are technically demanding. The simulations will be conducted at a constant temperature of 83 K where the LJ droplet, modelled based on an argon atom, remains in liquid state, while the substrate is a solid surface made up of cuprum atoms. The configurations are made up of an LJ droplet in interaction with the inner curve surface of a solid spherical and cylindrical shell. LJ droplets interacting with the outer curve surface of the solid substrate will not be investigated. The force field used in the MD simulation takes only a prototypical LJ form, namely  $V = 4\epsilon \left[ \left( \frac{\sigma}{r} \right)^{12} - \left( \frac{\sigma}{r} \right)^{6} \right]$ . The size of LJ nano droplets to be investigated is in the order of  $\sim 10^{1}$  nm. The range of LJ characteristic energy  $\epsilon$  to be investigated is in the order of  $\epsilon \sim \epsilon_{12, \mathrm{std}}$ , where  $\epsilon_{12, \mathrm{std}}$  is the  $\epsilon$  parameter in the standard LJ potential between the argon and cuprum elements.

#### 1.7 Thesis outline

This thesis consists of six chapters. Chapter One provides a general introduction, the research problem, objectives, contributions, and scope of the thesis. Chapter Two presents a comprehensive review of the literature on wetting phenomena related to the thesis scope. This chapter provides a review of the literature on wetting phenomena and its essential theoretical background. The discussion is implicit and aims to provide context for the MD simulation of LJ droplets in nano-wetting. Chapter Three covers a concise discussion on the theoretical background on classical theory of wetting and molecular dynamics simulation. Chapter Four describes the methodology used to conduct numerical experiments of nano wetting phenomena. Chapter Five presents the results obtained from the numerical experiments and discusses their implications. Finally, Chapter Six concludes the thesis by summarizing the findings, highlighting their significance, and providing recommendations for future research.

#### **CHAPTER 2**

#### LITERATURE REVIEW

#### 2.1 Introduction

This chapter provides a comprehensive explanation of MD simulation, which is a powerful tool used to study the behavior of particles at the molecular level. This chapter discusses the simulation in detail, including the LJ interaction potential, which is a common potential energy function used in MD simulations. Various methodologies used in MD simulations are also explored, along with their working theories, materials, geometries, advantages, and drawbacks.

One of the key topics covered in this chapter is the contact angle and its relationship to droplet size. The contact angle is an important parameter that characterizes the wetting behavior of a droplet on a surface. This chapter also presents a detailed analysis of the impact of droplet size on contact angle, based on a study of the literature. It highlights the use of MD simulation to predict the effects of interfacial tension and wetting mechanisms on nano-sized droplets deposited on diverse surfaces. Overall, this chapter will emphasize the importance of MD simulation in providing insights into the behavior of materials at the nanoscale. MD simulation is a valuable tool for understanding the properties and behavior of materials in various applications and built for variational method is a promising approach that can be used to predict and optimize the behavior of materials at the molecular level, which has important implications for a wide range of fields.

#### 2.2 Characterization of atomic behavior using MD simulation

MD simulation is a computational technique used to study the behavior of individual atoms or molecules in a system. By simulating the motions of particles

under various conditions, MD enables researchers to explore a wide range of phenomena in chemistry, materials science, and biophysics (Kolimi *et al.*, 2021). The scale at which MD simulations are performed can vary, with simulations typically divided into three categories: atomic scale, micro scale, and macro scale (Chen *et al.*, 2021). Through MD simulations, researchers can investigate a material's structure, mechanical properties, thermodynamic characteristics, and kinetic properties, among other features (Zhang and Banfield, 2014). These simulations are especially useful for studying systems that are difficult or impossible to observe experimentally, such as very small or very fast-moving particles (Hollingsworth and Dror, 2018). Fig. (2.1) provides a visual depiction of the different simulation techniques used in MD, highlighting the range of scales and phenomena that can be studied. Overall, MD simulations are a powerful tool for exploring the behavior of atoms and molecules in complex systems and have broad applications across many scientific disciplines (Xu *et al.*, 2021).

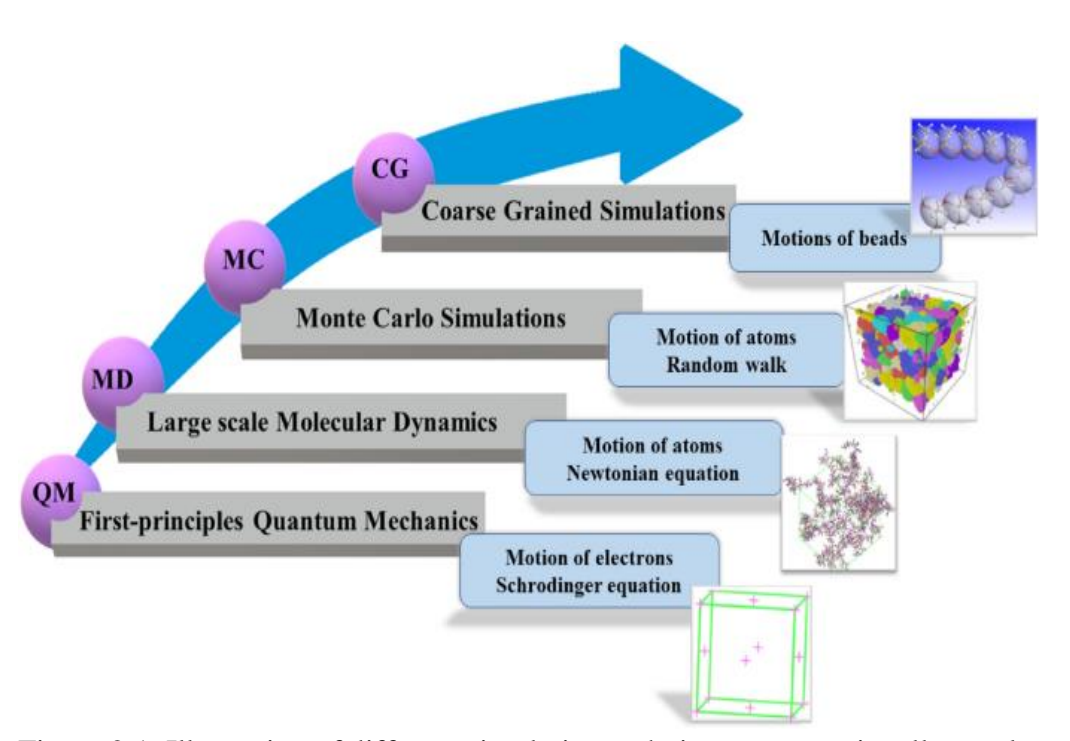


Figure 2.1. Illustration of different simulation techniques conventionally employed for simulating polymeric materials and their behavior (Sethi, 2022).

In the past, understanding the thermodynamic properties and behavior of a system required making assumptions based on theoretical models or experimental observations. However, with the advent of MD simulations, it is now possible to directly observe and simulate the movement of atoms and molecules in a liquid on solid substrates, as well as their interactions with each other (Di *et al.*, 2021).

By doing so, researchers can gain a deeper understanding of how droplets dynamically wet solid surfaces. MD simulations have proven to be a powerful tool for studying a wide range of physical and mechanical properties. For example, researchers can use MD simulations to estimate surface properties such as wetting, which is influenced by factors such as the size of droplets and the strength of interatomic potentials (Jiang *et al.*, 2017, Kanduč and Netz, 2017). By simulating these interactions at the atomic scale, researchers can then extrapolate their findings to larger scales and gain a better understanding of the behavior of the system (Blake and De Coninck, 2002).

Moreover, the ability to perform MD simulations has opened new avenues for research that were previously impossible or impractical. For instance, researchers can use MD simulations to test the effectiveness of new treatments or materials before implementing them in the lab. This can save time and resources, as well as provide valuable insights into the potential success or limitations of a particular approach. Overall, the use of MD simulations represents a significant advancement in our ability to study and understand complex systems. By providing a detailed and accurate picture of atomic-scale interactions, MD simulations offer a powerful tool for investigating a wide range of physical and mechanical properties, and for developing new treatments and materials (Blake and De Coninck, 2002, Di *et al.*, 2021).

In 2005, Hong *et al.* conducted a study using MD simulations to investigate the contact angle of non-polarized nanoscale argon droplets on a solid substrate. The contact angle refers to the angle formed between the surface of the liquid droplet and the surface of the solid substrate at the point where they meet. The researchers found that the size of the droplet played an important role in determining the contact angle, and that this relationship was related to the interaction between the liquid and the solid. Specifically, they found that when the liquid had a stronger interaction with the solid substrate, as would be the case for a more wetting liquid, the contact angle decreased as the droplet size decreased, and vice versa (Hong-Kai and Hai-Ping, 2005).

Luo and colleagues conducted a study recently, which was published in 2021. Using MD simulations, they aimed to investigate how nanoscale water droplets behave when in contact with various silica substrates. The results showed that the interaction potential energies between the water droplets and the substrates were crucial in determining the wetting behavior and contact angles. They found a wide range of contact angles, varying from 108.5° to 18.1°, depending on the strength of the interaction potential energies. The researchers also observed a clear transition from hydrophobic to hydrophilic behavior as the interaction potential energy between the water droplets and the substrates increased. This transition led to a significant improvement in the wettability of the substrate, which could have significant implications in materials science and engineering applications (Luo *et al.*, 2021).

Further, in 2020, a team of researchers led by Chen conducted MD simulations to explore the correlation between the characteristic energy of different flat surfaces and the intrinsic contact angle of water droplets. The team placed water molecules on various flat surfaces with varying characteristic energies and discovered that the intrinsic contact angle of the water droplets was influenced by the surface

characteristic energy. More specifically, they found that an increase in surface characteristic energy resulted in a decrease in the contact angle. This study emphasizes the crucial role of surface energy in determining the wetting behavior of liquid droplets on solid surfaces (Chen *et al.*, 2020).

Later, in the same year, a subsequent study by Hubao *et al.* provided additional insights into the impact of solid-liquid interaction strength on the wettability of substrates. Their findings indicated that as the interaction strength between the solid and liquid increased, the substrate underwent a transition from hydrophobic to hydrophilic behavior. Using a system consisting of two solid atoms and an oxygen atom, the researchers demonstrated the potential energy distribution perpendicular to the substrate surface under different strength potentials and the corresponding wetting status. The results, illustrated in Fig. (2.2), revealed that larger ( $\varepsilon_{O-S}$ ) values resulted in deeper potential energy wells and stronger hydrophilicity of the substrate. These findings could be of significant interest to researchers and engineers working in the field of materials science, as they demonstrate the potential to manipulate the wetting properties of substrates through careful control of solid-liquid interactions (Hubao *et al.*, 2020).

Moreover, Jiawei Di conducted a study in 2019 to investigate the movement of water droplets over substrates with different chemical compositions using MD simulations. The research involved analyzing the equivalent spreading radius and dynamic contact angle of the droplets, and the findings showed that the spreading process on chemically heterogeneous surfaces remained unaffected by the size of the droplet when it was sufficiently large. This implies that the droplet's diameter does not play a significant role in the spreading process under these conditions. The insights

gained from this study could be valuable for understanding and predicting the behavior of droplets on heterogeneous surfaces (Di *et al.*, 2019).

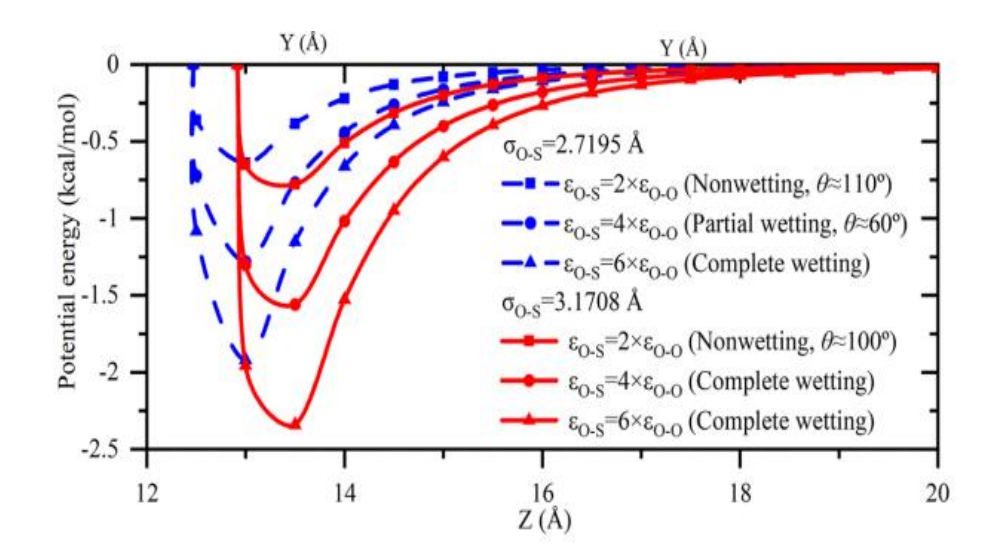


Figure 2.2. Potential energy field perpendicular to the substrate surface under different conditions (non-wetting, partial wetting, and complete wetting) (Hubao *et al.*, 2020).

The impact of the strength of fluid-solid interaction energy on the wettability of spherical particles was investigated in a 2018 study by Bhattarai and Priezjev using MD simulations and numerical minimization of interfacial energy. The study focused on wetting properties of composite interfaces that consist of a periodic array of rigidly attached spherical nanoparticles and a solid substrate. The researchers found that the strength of the liquid-solid interaction energy determined the local contact angle and therefore the wettability of the spherical particles. The results showed that the liquid film remained suspended at the surface of solid particles at zero applied pressure, and the distance to the solid substrate was determined by the particle radius and the local contact angle. Upon increasing external pressure, the liquid film was displaced closer to the solid substrate but remained stable up to a critical value due to the re-entrant curvature of the particle surface. The study's findings are essential for modeling partially wetting states on surfaces with multiple length scales of surface roughness (Bhattarai and Priezjey, 2018).

It is noteworthy that a study was conducted using MD simulation to investigate the evaporation and boiling behavior of a thin liquid layer on solid surfaces with different wettability characteristics, including hydrophilic, hydrophobic, and neutral surfaces. The research revealed that the rate of heat transfer from the solid surface to the liquid was significantly influenced by the surface wettability, as the likelihood of solid-liquid interaction increased. Moreover, the results indicated that hydrophilic surfaces exhibited a more efficient heat transfer compared to neutral and hydrophobic surfaces.

The study conducted by Shavik et al. can provide valuable insights for designing and optimizing heat transfer systems involving liquid-solid interfaces (Shavik et al., 2015). Similarly, the application of non-equilibrium MD simulations resulted in a significant enhancement in the rate of heat transfer from the substrate to the liquid by augmenting the chances of solid-liquid interaction potential, leading to increased surface wettability. This phenomenon was examined by investigating the influence of a thin argon liquid film on a solid substrate, which had been subject to various surface wetting conditions such as hydrophilic and hydrophobic, across a range of substrate materials, all at high wall superheat degrees. The study, conducted by Hasan et al. in 2017, delved into the impact of these conditions on the rate of heat transfer, with particular attention paid to the interplay between the liquid and solid interface. However, argon molecules have been also simulated with contact on the platinum surface at different solid-fluid combinations  $\frac{\varepsilon_{sf}}{\varepsilon}$  (at fixed  $\sigma_{sf}=0.9\sigma$ ) from 0.4 to 0.8, and at a temperature of 84 K. It was observed that with increasing the temperature, spreading rate of the argon droplet is increasing, and the contact angle decreases. While with decreasing solid-liquid interaction potential, contact angle will increase (Hasan et al., 2017).

#### 2.3 Different computational approaches

One of the most well-established simulation methods for evaluating the wetting properties of materials is solid-liquid-vapor systems. These simulations involve studying the behavior of particles at the interface of the solid, liquid, and vapor phases. In recent years, a class of simulation techniques has emerged that focuses on particle wetting and de-wetting from liquid drops or bubbles. These techniques have been used to investigate the wetting characteristics of a range of materials, including hydrophobic and hydrophilic surfaces (Amabili *et al.*, 2018).

In this work, we will discuss many studies based on different simulation techniques including Monte Carlo (MC) and MD simulation. Principle-based simulation can offer the most trustworthy way to establish a theoretical constraint for predicting material characteristics. Which are based on droplet geometries and free energies, respectively (Jiang and Patel, 2019). In general, according to the distribution of the systems, the two primary subcategories of molecular simulation techniques are MD and MC.

In MD techniques, the system's dynamical trajectory is produced by numerically integrating the equations of motion (Newton's equations) are numerically simulated to produce the trajectory of a molecule's dynamics with time (Groenhof, 2013). It can be used to examine the system's structural, dynamic, and thermodynamic characteristics. As well as Fixed-charge force fields (FFs) are commonly utilized in MD simulations of concentrated systems (Riniker, 2018, Nerenberg and Head-Gordon, 2018). They are made up of a few parameters, such as bond-stretching, bond-angle bending, and LJ parameters (Böselt *et al.*, 2021). While, in MC techniques, another configuration is created by using probabilistic rules, and this process is applied

to create a sequence of states that can be used to calculate structural and thermodynamic properties but not dynamical properties because MC simulations don't even have a concept of time. As a result, the MC method in which produces the dynamics are not the system's temporal dynamics. Conversely, the collection of configurations can be reflected from those dynamically evaluated (Grossfield *et al.*, 2018).

Although, MC or MD simulations can be used to describe the droplet geometries and free energies. Whereby, a liquid droplet is performed, and contact angles are determined from a droplet shape characterization. Similarly, line tension, interfacial curvature, or a slightly random selection of the solid-fluid contact plane. employing enormous cylindrical droplets, sometimes with changing droplet diameters (Jiang and Patel, 2019, Lu *et al.*, 2019). Additionally, molecules are represented in molecular mechanics (MM) by particles that are made up of individual atoms or groups of atoms. With many empirical parameters, fit to experiment or other data used to compute non-bonded and bound interactions, each atom may be given an electric charge and a potential energy function. But, because it cannot mimic bond rearrangements, that's why MM is often not too accurate. Thus, averaged characteristics are obtained in classical simulations by ignoring electron rearrangement (Böselt *et al.*, 2021).

On the other hand, to represent electronic modifications during a chemical reaction, a quantum mechanical (QM) description is necessary for those elements of the system that are engaged in the reaction (Groenhof, 2013, Bottaro and Lindorff-Larsen, 2018). QM electrons are expressly included in the model, and interaction energy is estimated by resolving the electronic structure of the system's molecules with

a few empirical constants. It's a strong tool for forecasting the inherent wettability and wettability modification properties of multi-phase systems seen in nature as well as in other energy-liquid applications. However, QM simulations also may be too computationally costly to allow simulations of the time and length scales necessary to characterize the system of interest (Lu *et al.*, 2017, Bottaro and Lindorff-Larsen, 2018). However, the wetting can be described in quantum mechanics using a hybrid scheme that combines MM and QM. It has been alteration of surface wettability in multiphase systems at high temperatures. Using this method offers a novel way to investigate the mechanism of complex wetting events in multiphase systems (Lu *et al.*, 2019). The wetting characteristics of crystalline surfaces for a range of polar or nonpolar liquids have been demonstrated using QM for polar and thermal effects. QM was directly applied to multiphase systems to understand the mechanisms behind complex surface wetting and interfacial behaviors, particularly polar interactions. Moreover, this QM technique is universal and may be used with any crystal surface and a variety of surrounding fluids (Lu *et al.*, 2019).

In 2018, scientists utilized density functional theory (DFT) in QM simulations to assess how the adsorption of pure water affects the surface wettability of graphite. The objective was to estimate the macroscopic surface wettability of graphite without considering any experimental features such as water surface tensions. By utilizing the DFT approach, the study aimed to provide a more direct evaluation of the impact of water adsorption on the surface wettability of graphite. The researchers concluded that the DFT approach was effective in achieving this objective (Lu *et al.*, 2018). Moreover, MD simulations are frequently used to explore interfacial properties, including the interaction between surfactants and water, as well as interface thickness. This aids in understanding how molecular structure can influence interfacial tension.

Subsequently, QM analysis is utilized to investigate the polarity of the system, which allows for a more detailed examination of the interaction between the headgroup and water molecules. By combining these two computational approaches, a comprehensive understanding of the interfacial behaviour and its underlying molecular mechanisms can be achieved. (Xu *et al.*, 2013).

Bourasseau *et al.* employed the MC simulation method to calculate the surface tension of a substance. While the results were less dispersed than experimental data, indicating that MC simulations are relatively easy to perform, the researchers found that the high level of agreement between their analytical findings and the experimental data was primarily due to the potential used in the simulations. In their study, they compared different potential models and showed that selecting the right potential is crucial for achieving accurate results in MC simulations (Bourasseau *et al.*, 2013).

A water droplet on graphene was investigated by Taherian and colleagues through quantum molecular dynamics (QMD) simulations, yielding a contact angle of 87°. While proposing that the line tension might have been greatly influenced by the limited number of molecules, with only 125 water molecules being utilized in the droplet for these calculation (Taherian *et al.*, 2013). One notably challenges with nanodroplets from MD simulations is that the conventional  $\theta$  becomes diverse, especially at the molecular level. However, different methods to approximately fit the outline of a droplet onto a spherical shape have been utilized (Fan and Cağin, 1995, Hirvi and Pakkanen, 2006, Hirvi and Pakkanen, 2007, Do Hong *et al.*, 2009).

A significant hurdle in relating MD simulations to experimental outcomes is the absence of a uniform protocol for creating the droplet or the surface, and varying initial conditions can result in a vast divergence of the obtained values. For instance,  $\theta$  values of water on graphene obtained from both simulations and experiments display a wide range, varying from 29° to 115°. The most frequently reported range is between 84°-86°, indicating that the interpretation of the results from different studies can be challenging. Hence, it is crucial to establish a consistent methodology for the creation of both the droplet and the surface to facilitate a more precise correlation between simulation and experimental outcomes. This, in turn, can aid in the development of a more comprehensive understanding of the behavior of nanodroplets at the molecular level, and the factors that influence their interaction with surfaces (Mattia, 2007).

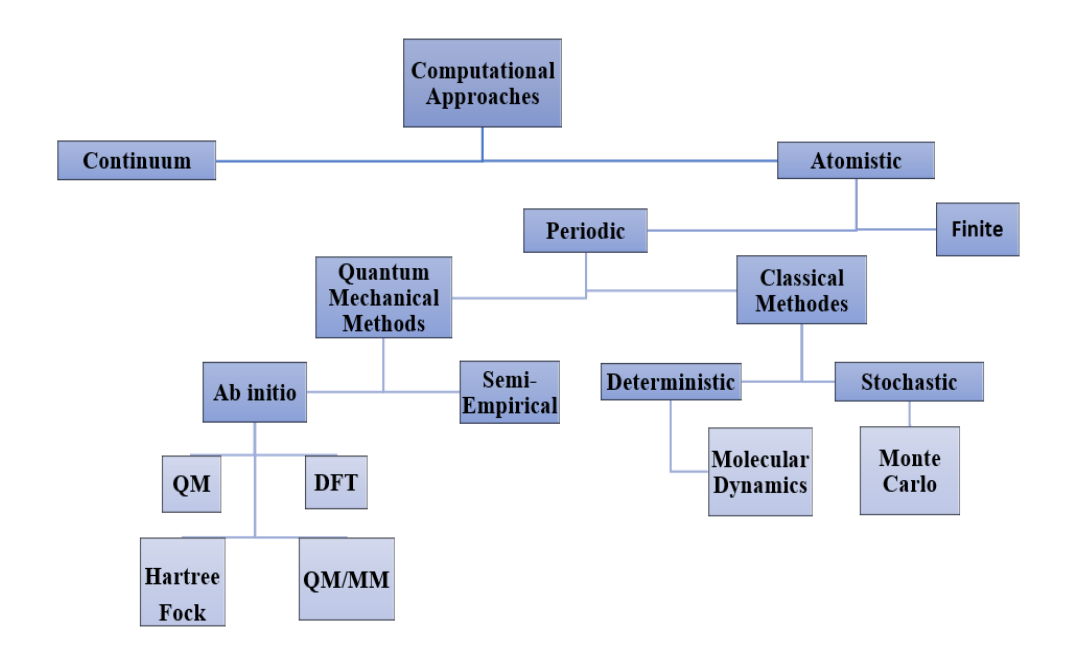


Figure 2.3. Hierarchy chart of computational approaches.

#### 2.4 Contact-angle and wetting characterization of triple surfaces

The contact angle is the angle on the droplet side of a line drawn through the three-phase boundary and tangent to the liquid-vapor interface as shown in Fig. (2.4). There are various sorts of contact angles, including "ideal contact angle" which is for an ideal material with drops having radii of curvature larger than nanometric size.